Joint Secrecy and Latency Performance Analysis for UAV-Assisted Uplink NOMA-Based IoT Network with Mobile Edge Computing

Quoc-Huy Nguyen-Anh[1,2], Anh-Nhat Nguyen[3], and Dac-Binh Ha[1,2(✉)]

[1] Faculty of Electrical-Electronic Engineering, Duy Tan University, Da Nang 550000, Vietnam
hadacbinh@duytan.edu.vn
[2] Institute of Research and Development, Duy Tan University, Da Nang 550000, Vietnam
[3] Department of Computing Fundamentals, FPT University, Hanoi 10000, Vietnam
nhatna3@fe.edu.vn

Abstract. This study jointly investigates the secrecy and latency performance of uplink nonorthogonal multiple access (NOMA)-based mobileedge computing (MEC) Internet of Things (IoT) system employing unmanned aerial vehicle (UAV). Specifically, this proposed system consists of two resource-limited edge devices (ED) that seek to offload their tasks to a UAV equipped with one MEC server in the presence of a passive eavesdropper. To evaluate the system's secrecy and latency performance, we derive the closed-form expressions of secrecy successful computation probability (SSCP) and its upper bound. The Monte Carlo simulation results supported the accuracy of our study based on computer simulations according to various system parameters such as the average transmit signal-to-noise ratio (SNR), power allocation ratio, and altitude of UAV.

Keywords: Internet of Things · unmanned aerial vehicles · nonorthogonal multiple access · mobile edge computing · physical layer secrecy

1 Introduction

The need for mobile data traffic in the field of Internet of Things (IoT) has experienced a significant surge in recent years. Nevertheless, the mobile terminal, which is limited in energy and computational capacity, faces challenges in accommodating the increasing demand for applications that rely on sustained and intensive calculations. Examples of such applications include virtual and augmented reality, remote operations, and autonomous driving [1]. To address these issues, researchers have proposed two potential strategies for IoT

N.-S. Vo et al. (Eds.): INISCOM 2024, LNICST 595, pp. 236–255, 2024.
https://doi.org/10.1007/978-3-031-67357-3_17

networks, namely mobile-edge computing (MEC) and nonorthogonal multiple access (NOMA) [2]. The primary concept behind MEC is to leverage the existing computational resources in the vicinity to enable mobile terminals to do computations. On the other hand, NOMA enables several mobile terminals to communicate in the power domain by utilizing the same time/frequency resource block. NOMA is characterized by the necessity of employing superposition coding during the transmission phase and successive interference cancellation (SIC) during the reception phase [3]. MEC generally provides two compute offloading modes, namely partial offloading and binary offloading [4]. Furthermore, recent studies have examined the integration of NOMA-based MEC systems in order to improve the efficiency of offloading [5,6]. The study conducted in reference [5] examined two distinct offloading scenarios based on NOMA technology. The study conducted in [6] examined a MEC system that utilizes NOMA and consists of two clusters of edge devicess (EDs) connected through a multiantenna access point (AP).

Nevertheless, the effectiveness of MEC is heavily reliant on the transfer of data and computational processes that occur between devices and servers. The efficacy of signal reception can be compromised due to the arbitrary positioning of EDs. The bulk of EDs have low power characteristics, which consequently restricts their transmission range. The utilization of wireless communication with UAV is a possible technological solution to address the aforementioned shortcomings [7]. A distinguishing feature of UAV communication lies in the presence of Line-of-Sight (LoS) connections. These links offer several advantages, including reduced small-scale fading, potential improvements in network performance, and the capacity for UAV to provide signal coverage. This feature has been highlighted in previous research [8]. Moreover, UAV have the capability to approach EDs at a proximity that ensures the establishment of dependable communication connections. Hence, a UAV has the capability to serve as flexible and reliable transport mechanisms when integrated with edge servers [9], or act as links between devices such as EDs, a base station (BS), or an AP [10].

Furthermore, the susceptibility of tasks offloaded by EDs to MEC servers across wireless channels to interception by hostile eavesdroppers gives rise to concerns regarding information leakage. Hence, it is imperative to assess the security of the MEC system. The concept of physical-layer security (PLS) is based on using the inherent properties of wireless channels in order to provide secure transmission. This area of research has received significant attention in the field of wireless communication systems. Attaining total security is deemed unachievable [11] because to the unavailability of channel state information (CSI) pertaining to the eavesdropper at the transmitter, as well as the presence of tight delay limits in certain systems. Multiple researches have investigated the NOMA-based MEC technology, specifically focusing on PLS. In [12], the study assumes that eavesdropper CSI follows a bounded channel uncertainty model. It aims to optimize the secure energy efficiency in NOMA-based massive machine-type communication (mMTC) networks while ensuring that the latency requirements of terminal devices are met. In [13], the authors initially sought to minimize

the overall energy consumption of users, taking into account several limitations such as secure offloading rate, computation time, and secrecy outage probability. Subsequently, they further decreased this energy consumption by incorporating the priorities of two users.

This study investigates the performance of secrecy offloading in IoT networks that utilize UAV-assisted NOMA-MEC across Nakagami-m fading channels. Furthermore, we take into account the likelihood of LoS and non-LoS (NLoS) scenarios in wireless channels between UAV and ground devices. In addition, we examine the performance of the system in terms of secrecy offloading, taking into account the presence of imperfect CSI (iCSI) between the UAV and the EDs. Our main contributions are as follows:

- We investigate a UAV-assisted NOMA-MEC with passive eavesdropping for IoT networks. Furthermore, we consider iCSI to obtain accurate evaluations of the secrecy offloading performance of the system in practice. Accordingly, we propose an offloading protocol based on uplink NOMA scheme.
- We derive the closed-form expression of SSCP for the entire system. In addition, in order to reduce the computing complexity, we also derive an upper-bound expression for the SSCP.
- We utilize the derived expressions to evaluate the impact of key parameters to secrecy and latency performance of our proposed system. Finally, all analytic expressions are validated by computer simulations.

The remainder of this paper is organized as follows. In Sect. 2, the system model and communication protocol are introduced. In Sect. 3, the SSCP and its upper bound are analyzed. In Sect. 4, numerical results are presented and discussed. Finally, Sect. 5 is our conclusions.

2 System Model and Communication Protocol

2.1 System and Channel Model

As shown in Fig. 1, we investigate a UAV-assisted NOMA-MEC-based IoT network with two edge devices A and B, where A and B are the far-near devices. Because these two devices are limited in resources, they intend to offload confidential tasks to the UAV-equipped MEC server, denoted by U, while passive eavesdroppers (without any attacks) are present nearby, denoted as E. We assume all devices operate with a single antenna in half-duplex mode, within an urban environment.

Without loss of generality, we utilized a 3D Cartesian coordinate system, we use $U\left(x_U, y_U, h_U\right)$, where $h_U > 0$; $A\left(x_A, y_A, 0\right)$; $B\left(x_B, y_B, 0\right)$; and $E\left(x_E, y_E, 0\right)$. Assuming that the large-scale attenuation of the channel between the UAV and EDs is governed by a LoS and NLoS probability models. When considering the probability of both LoS and NLoS connections between the UAV and all ground devices, the mean path loss is calculated as follows [14]:

$$\mathcal{L}_{ab}\left(d_{ab}, \varphi_{ab}\right) = \left[\mathcal{K}_{NLoS} + \frac{\mathcal{K}_{LoS} - \mathcal{K}_{NLoS}}{1 + \mathcal{B}e^{\left(-\frac{180}{\pi}\mathcal{A}\varphi_{ab} + \mathcal{A}\mathcal{B}\right)}}\right] d_{ab}^{\sigma}, \tag{1}$$

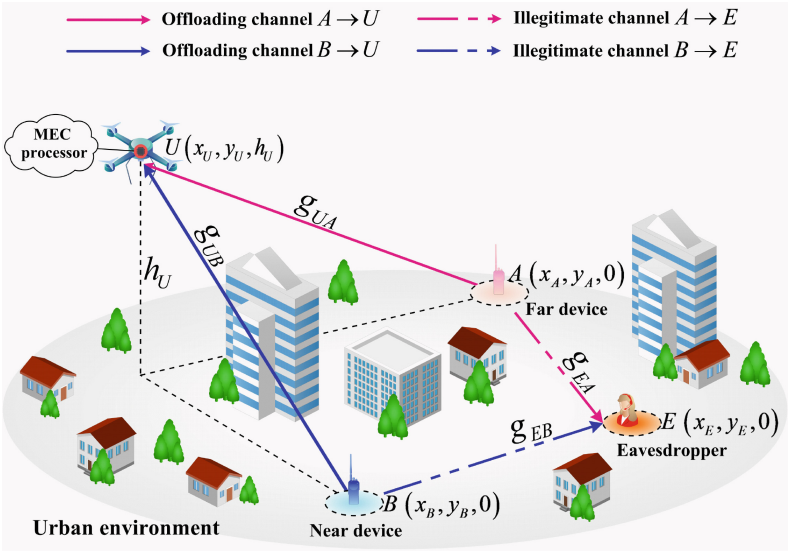

Fig. 1. System model for a UAV NOMA-MEC in IoT network.

where $ab \in \{UA, UB\}$, the elevation angle $\varphi_{ab} = \arcsin\left(\frac{h_U}{d_{ab}}\right)$ and the distance from a to b is denoted $d_{ab} = \sqrt{(x_b - x_a)^2 + (y_b - y_a)^2 + {h_U}^2}$; σ is the path-loss exponent; $\mathcal{A}$ and $\mathcal{B}$ are constants depending on the surrounding environment; and $\mathcal{K}_l = \mathcal{O}_l(c/4\pi f_c)^{-1}$ is parameters depend on the environment, terrain, and carrier frequency, where $l \in \{LoS, NLoS\}$, c is the speed of light when traveling through air, f_c is the carrier frequency, and $\mathcal{O}_l$ is the excessive path losses of both LoS and NLoS transmission processes. Assume that all EDs execute the same task of length L (bits) and are classified [6]. The capacity offload of A and B can thus be written as follows:

$$L_I^{off} = \beta_I L, \tag{2}$$

where $I \in \{A, B\}$ and $\beta_I, 0 \leq \beta_I \leq 1$ stands for the offloading ratio. The channel coefficients from the $I \rightarrow U$ and $I \rightarrow E$ are denoted by g_{IU} and g_{IE}, respectively. The attainment of perfect CSI in wireless systems is a challenging task due to the presence of mistakes in channel estimates and delays in feedback. Hence, the channel coefficient is expressed as follows [2]:

$$g_\psi = \hat{g}_\psi + e_\psi, \tag{3}$$

where $\psi \in \{IU, IE\}$; $\hat{g}_\psi$ is the estimated channel coefficient and $e_\psi \sim \mathcal{CN}(0, \delta_\psi)$ denotes the channel estimation error, which can be approximated as a Gaussian distribution, where the parameter δ_ψ indicates the quality of channel estimation. In this paper, it is assumed that the channel estimation error variance δ_ψ is constant [15,16]. We assume that all channels are modeled as Nakagami-m

fading channels and that the channel coefficients are random variables (RVs) distributed following the Nakagami-m model [2]. Thus the cumulative distribution function (CDF) and probability density function (PDF) of channel power gains are respectively expressed as:

$$F_{|\hat{g}_\psi|^2}(y) = 1 - e^{-\frac{my}{\lambda_\psi}} \sum_{s=0}^{m-1} \frac{1}{s!} \left(\frac{my}{\lambda_\psi}\right)^s, \tag{4}$$

$$f_{|\hat{g}_\psi|^2}(y) = \frac{m^m y^{m-1}}{\lambda_\psi^m (m-1)!} e^{-\frac{my}{\lambda_\psi}}, \tag{5}$$

where λ_ψ stands for the average channel power gain.

2.2 Communication Protocol

In this subsection, we delineate the communication protocol of the proposed system. Figure 2 illustrates the timing diagram of the protocol and is described as follows.

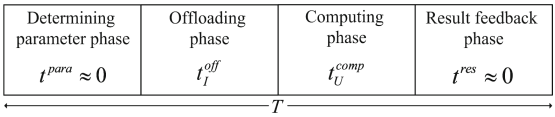

Fig. 2. Time flowchart of the considered UAV NOMA-MEC network.

- The first phase, t^{para}: U sends pilot signals to $\{A, B\}$ and collects CSI of all connections.
- The second phase, t_I^{off}: A and B deploy the uplink NOMA scheme to offload their tasks to U. Thus, the received signal at U is as follows:

$$y_U^{MEC} = \sqrt{\frac{\rho P_S}{\mathcal{L}_{AU}}} (\hat{g}_{AU} + e_{AU}) x_A + \sqrt{\frac{(1-\rho) P_S}{\mathcal{L}_{BU}}} (\hat{g}_{BU} + e_{BU}) x_B + n_U, \tag{6}$$

where x_A and x_B are the respective offloaded signals of A and B; P_S is the transmission power of EDs; ρ represents the power allocation coefficient, $0.5 < \rho \leq 1$; $n_U \sim \mathcal{CN}(0, N_0)$ is additive white Gaussian noise (AWGN). U decodes x_A and x_B based on SIC [3]. Therefore, the signal-to-interference-plus-noise ratios (SINRs) received at the U for detecting x_A and x_B are represented as follows:

$$\gamma_{UA}^{x_A} = \frac{\gamma_1 |\hat{g}_{AU}|^2}{\gamma_2 |\hat{g}_{BU}|^2 + \gamma_3}, \tag{7}$$

$$\gamma_{UB}^{x_B} = \frac{\gamma_2 |\hat{g}_{BU}|^2}{\gamma_2 \delta_{BU} + 1}, \tag{8}$$

where $\gamma_1 = \frac{\rho\gamma_I}{\mathcal{L}_{AU}}$, $\gamma_2 = \frac{(1-\rho)\gamma_I}{\mathcal{L}_{BU}}$, $\gamma_I = \frac{P_S}{N_0}$, and $\gamma_3 = \gamma_1\delta_{AU} + \gamma_2\delta_{BU} + 1$. Similarly, the expression of signal received at E is as follows:

$$y_E = \sqrt{\frac{\rho P_E}{d_{AE}^{\sigma}}}\left(\hat{g}_{AE} + e_{AE}\right)x_A + \sqrt{\frac{(1-\rho)\,P_E}{d_{BE}^{\sigma}}}\left(\hat{g}_{BE} + e_{BE}\right)x_B + n_E, \quad (9)$$

where $n_E \sim \mathcal{CN}(0, N_E)$ is AWGN at E. We suppose E also applies SIC, similarly, the SINR to detect x_A and x_B at E is given by

$$\gamma_{EA}^{x_A} = \frac{\gamma_4|\hat{g}_{AE}|^2}{\gamma_5|\hat{g}_{BE}|^2 + \gamma_6}, \quad (10)$$

$$\gamma_{EB}^{x_B} = \frac{\gamma_5|\hat{g}_{BE}|^2}{\gamma_5\delta_{BE} + 1}, \quad (11)$$

where $\gamma_4 = \frac{\rho\gamma_E}{d_{AE}^{\sigma}}$, $\gamma_5 = \frac{(1-\rho)\gamma_E}{d_{BE}^{\sigma}}$, $\gamma_E = \frac{P_E}{N_E}$, and $\gamma_6 = \gamma_4\delta_{AE} + \gamma_5\delta_{BE} + 1$.

– In the third phase, t_U^{comp}: The server at U computes the offloaded tasks. The time required to complete the computation of the number of bits of the task at U is as follows:

$$t_U^{comp} = \frac{\left(L_A^{off} + L_B^{off}\right)\varsigma}{f_U^{MEC}}, \quad (12)$$

where ς represents the number of CPU cycles required to execute one input bit, and f_U^{MEC} stands for the operating frequency of MEC at U.

– In the fourth phase, t^{res}: U sends computed data results to I. The return latency of results from U to I is neglected since the returned results are significantly smaller than the offloaded data [6].

2.3 Time Offloading and Secrecy Capacity

The instantaneous capacity of the legitimate channel from the $I \rightarrow U$ link is computed as follows:

$$C_{IU}^{x_I} = W\log_2\left(1 + \gamma_{IU}^{x_I}\right), \quad (13)$$

where W represents the bandwidth. Hence, the time offloading from I to U is given by

$$t_I^{off} = \frac{L_I^{off}}{C_{IU}^{x_I}}. \quad (14)$$

The instantaneous secrecy capacity of wireless communication channel from I to U in the presence of a passive eavesdropper is defined as follows [17]:

$$\begin{aligned} C_I^{Sec} &= \left[C_{IU}^{x_I} - C_{IE}^{x_I}\right]^+ \\ &= \begin{cases} W\log_2\left(\frac{1+\gamma_{IU}^{x_I}}{1+\gamma_{IE}^{x_I}}\right), & \gamma_{IU}^{x_I} > \gamma_{IE}^{x_I} \\ 0, & \gamma_{IU}^{x_I} \leq \gamma_{IE}^{x_I} \end{cases}, \end{aligned} \quad (15)$$

where $C_{IE}^{x_I} = W\log_2\left(1 + \gamma_{IE}^{x_I}\right)$ is the illegal channel capacity.

3 Performance Analysis

3.1 Secrecy Successful Computation Probability (SSCP)

In this subsection, we present the joint secrecy and latency performance analysis of the proposed system in terms of SSCP [18], denoted by $\mathcal{S}$. The $\mathcal{S}$ is defined as the probability that all offloading tasks are completed within the maximum permissible system latency T^{th} and the corresponding secrecy capacity is greater than a predefined data rate threshold R_S. Thus, the expression expressing the performance of the entire system is calculated as follows:

$$\mathcal{S} = \Pr\left(t_A^{off} < T^{th}, t_B^{off} < T^{th}, C_A^{Sec} > R_S, C_B^{Sec} > R_S\right), \tag{16}$$

where $T^{th} = T - t_U^{comp}$.

Theorem 1. *The closed-form expression for the SSCP of the entire system for UAV-aided NOMA-MEC under quasi-static Nakagami-m fading is as follows:*

$$\mathcal{S} = \mathcal{C}\left(\mathcal{I}_{31} - \mathcal{I}_{32} - \mathcal{I}_{33}\right), \tag{17}$$

where $\mathcal{C} = \frac{m_A^{m_A}}{\lambda_A^{m_A}(m_A-1)!}\frac{m_B^{m_B}}{\lambda_B^{m_B}(m_B-1)!}\frac{m_{BE}^{m_{BE}}}{\lambda_{BE}^{m_{BE}}(m_{BE}-1)!}$; $\mathcal{I}_{31}$, $\mathcal{I}_{32}$ *and* $\mathcal{I}_{33}$ *are defined as follows:*

$$\begin{aligned}\mathcal{I}_{31} &= (m_{BE}-1)!\left(\frac{m_{BE}}{\lambda_{BE}}\right)^{-m_{BE}}\sum_{j_1=0}^{m_A-1}\sum_{k_1=0}^{j_1}\sum_{k_2=0}^{m_B+k_1-1}\frac{(m_B+k_1-1)!}{k_2!k_1!(j_1-k_1)!}\\ &\times (m_A-1)!\left(\frac{m_A}{\lambda_A}\right)^{-(m_A-j_1)}\left(\frac{v_3}{v_2}\right)^{j_1-k_1}\left(\frac{m_A v_2}{\lambda_A}+\frac{m_B}{\lambda_B}\right)^{-(m_B+k_1-k_2)}\\ &\times {v_2}^{j_1}{v_1}^{k_2}e^{-v_1\left(\frac{m_A v_2}{\lambda_A}+\frac{m_B}{\lambda_B}\right)-\frac{m_A v_3}{\lambda_A}},\end{aligned} \tag{18}$$

$$\begin{aligned}\mathcal{I}_{32} &= \sum_{i_2=0}^{m_{BE}-1}\sum_{j_1=0}^{m_A-1}\sum_{k_1=0}^{j_1}\sum_{k_3=0}^{i_2}\sum_{k_4=0}^{m_B+k_1+k_3-1}\left(\frac{m_{BE}}{\lambda_{BE}}\right)^{-(m_{BE}-i_2)}\left(\frac{m_A}{\lambda_A}\right)^{-(m_A-j_1)}\\ &\times\frac{(m_A-1)!\,(m_{BE}-1)!\,(m_B+k_1+k_3-1)!}{k_1!k_3!k_4!(j_1-k_1)!(i_2-k_3)!}\left(\frac{v_3}{v_2}\right)^{j_1-k_1}\left(\frac{v_5}{v_4}\right)^{i_2-k_3}\\ &\times\left(\frac{m_{BE}v_4}{\lambda_{BE}}+\frac{m_A v_2}{\lambda_A}+\frac{m_B}{\lambda_B}\right)^{-(m_B+k_1+k_3-k_4)}{v_1}^{k_4}{v_2}^{j_1}{v_4}^{i_2}\\ &\times e^{-\left(\frac{m_{BE}v_4}{\lambda_{BE}}+\frac{m_A v_2}{\lambda_A}+\frac{m_B}{\lambda_B}\right)v_1+\frac{m_{BE}v_5}{\lambda_{BE}}+\frac{m_A v_3}{\lambda_A}},\end{aligned} \tag{19}$$

$$\mathcal{I}_{33} = \frac{\pi^2}{4QR} \sum_{i_1=0}^{m_{AE}-1} \sum_{i_3=0}^{i_1} \sum_{r=1}^{R} \sum_{q=1}^{Q} \left(\frac{m_{AE}}{\lambda_{AE}}\right)^{i_1} \left(\frac{\gamma_6}{\gamma_5}\right)^{i_1-i_3} (\theta_q)^{m_B-1} \left(\theta_o^{(\theta_q)}\right)^{m_A-1}$$
$$\times \frac{(m_{BE}+i_3-1)!\sqrt{1-\zeta_q{}^2}\sqrt{1-\zeta_o{}^2}}{i_3!\,(i_1-i_3)!} \omega_q{}^{\frac{m_B}{\lambda_B}-1} \left(\omega_o^{(\theta_q)}\right)^{\frac{m_A}{\lambda_A}-1}$$
$$\times \left(\Xi_1^{\left(\theta_q,\theta_o^{(\theta_q)}\right)}\right)^{i_1} \left(\Xi_3^{\left(\theta_q,\theta_o^{(\theta_q)}\right)}\right)^{-(m_{BE}+i_3)} e^{-\frac{m_{AE}}{\lambda_{AE}}\Xi_2^{\left(\theta_q,\theta_o^{(\theta_q)}\right)}-(v_2\theta_q+v_3)}$$
$$\times \left[1 - e^{-\Xi_3^{\left(\theta_q,\theta_o^{(\theta_q)}\right)}(v_4\theta_q+v_5)} \sum_{i_4=0}^{m_{BE}+i_3-1} \frac{1}{i_4!}(v_4\theta_q+v_5)^{i_4} \left(\Xi_3^{\left(\theta_q,\theta_o^{(\theta_q)}\right)}\right)^{i_4}\right], \tag{20}$$

which $\theta_A = 2^{\frac{L_A^{off}}{WT^{th}}} - 1$, $\theta_B = 2^{\frac{L_B^{off}}{WT^{th}}} - 1$, $\varphi_S = 2^{\frac{R_S}{W}}$, $v_1 = \frac{\theta_B(\gamma_2\delta_{BU}+1)}{\gamma_2}$, $v_2 = \frac{\theta_A\gamma_2}{\gamma_1}$, $v_3 = \frac{\theta_A\gamma_3}{\gamma_1}$, $v_4 = \frac{\gamma_2(\gamma_5\delta_{BE}+1)}{\gamma_5\varphi_S(\gamma_2\delta_{BU}+1)}$, $v_5 = \frac{(1-\varphi_S)(\gamma_5\delta_{BE}+1)}{\gamma_5\varphi_S}$. *Note that,* $\Xi_1^{\left(\theta_q,\theta_o^{(\theta_q)}\right)}$, $\Xi_2^{\left(\theta_q,\theta_o^{(\theta_q)}\right)}$, *and* $\Xi_3^{\left(\theta_q,\theta_o^{(\theta_q)}\right)}$ *are defined as follows:*

$$\Xi_1^{\left(\theta_q,\theta_o^{(\theta_q)}\right)} = \left(\frac{\gamma_1\theta_o^{(\theta_q)}}{\gamma_2\theta_q+\gamma_3} + 1 - \varphi_S\right)\frac{\gamma_5}{\gamma_4\varphi_S}, \tag{21}$$

$$\Xi_2^{\left(\theta_q,\theta_o^{(\theta_q)}\right)} = \left(\frac{\gamma_1\theta_o^{(\theta_q)}}{\gamma_2\theta_q+\gamma_3} + 1 - \varphi_S\right)\frac{\gamma_6}{\gamma_4\varphi_S}, \tag{22}$$

$$\Xi_3^{\left(\theta_q,\theta_o^{(\theta_q)}\right)} = \frac{m_{AE}\Xi_1^{\left(\theta_q,\theta_o^{(\theta_q)}\right)}}{\lambda_{AE}} + \frac{m_{BE}}{\lambda_{BE}}, \tag{23}$$

where $\zeta_q = \cos\left(\frac{\pi(2q-1)}{2Q}\right)$, $\omega_q = \frac{(\zeta_q+1)e^{-v_1}}{2}$, $\theta_q = -\ln(\omega_q)$, $\zeta_o = \cos\left(\frac{\pi(2r-1)}{2R}\right)$, $\omega_o^{(\theta_q)} = \frac{(\zeta_o+1)e^{-(v_2\theta_q+v_3)}}{2}$, $\theta_o^{(\theta_q)} = -\ln\left(\omega_o^{(\theta_q)}\right)$ *with* R *and* Q *are the complexity versus accuracy trade-off coefficient [19].*

Proof. See Appendix A.

3.2 Upper Bound

In this subsection, we discuss the upper bound of the SSCP. It is necessary to conduct an upper-bound analysis to assess how various system parameters impact the performance of the SSCP [20].

Theorem 2. *The upper bound expression for the SSCP of the entire system for UAV-aided NOMA-MEC under quasi-static Nakagami-m fading is as follows:*

$$\mathcal{S}_{upper} = \frac{1}{(m_B-1)!}\left(\frac{m_B}{\lambda_B}\right)^{m_B}\frac{\pi}{K}\sum_{k=0}^{K}\sqrt{\frac{1-v_k}{1+v_k}}(-\ln(t_k))^{m_B-1}t_k{}^{\frac{m_B}{\lambda_B}} \times \Upsilon_1, \quad (24)$$

where $v_k = \cos\left(\frac{\pi(2k-1)}{2K}\right)$, $t_k = \frac{d(v_k+1)}{2}$, $d = e^{-v_1}$, *and* K *is the complexity versus accuracy trade-off coefficient [19];* Υ_1 *is defined as follows:*

$$\begin{aligned}
\Upsilon_1 &= e^{-\frac{m_A}{\lambda_A}(v_2(-\ln t_k)+v_3)}\sum_{i_5=0}^{m_A-1}\frac{1}{i_5!}\left(\frac{m_A}{\lambda_A}(v_2(-\ln t_k)+v_3)\right)^{i_5}\Bigg[1-t_k{}^{\frac{m_{BE}}{\lambda_{BE}}a_7} \\
&\times\sum_{i_3=0}^{m_{BE}-1}\frac{1}{i_3!}\left(\frac{m_{BE}}{\lambda_{BE}}a_7(-\ln t_k)\right)^{i_3}\Bigg]-\left(\frac{1}{(m_A-1)!}\right)\left(\frac{1}{(m_{BE}-1)!}\right) \\
&\times\left(\frac{m_A}{\lambda_A}\right)^{m_A}\left(\frac{m_{BE}}{\lambda_{BE}}\right)^{m_{BE}}\frac{\pi}{R}\sum_{i_1=0}^{m_{AE}-1}\sum_{i_2=0}^{i_1}\sum_{r=0}^{R}\frac{\sqrt{1-v_q}}{\sqrt{1+v_q}}C_{i_2}^{i_1}\frac{1}{i_1!}\left(\frac{a_4}{a_3}\right)^{i_1-i_2} \\
&\times\left(\frac{m_{AE}}{\lambda_{AE}}\left(\frac{a_3}{a_5(-\ln t_k)+a_6}\right)\right)^{i_1}t_{q\,k}{}^{\frac{m_{AE}a_4}{\lambda_{AE}a_5(-\ln t_k)+\lambda_{AE}a_6}+\frac{m_A}{\lambda_A}}(-\ln t_{q_k})^{i_1+m_A-1} \\
&\times\Bigg[(i_2+m_{BE}-1)!\left(\frac{m_{AE}a_3(-\ln t_{q_k})}{\lambda_{AE}a_5(-\ln t_k)+\lambda_{AE}a_6}+\frac{m_{BE}}{\lambda_{BE}}\right)^{-i_2-m_{BE}} \\
&-t_k{}^{\left(\frac{m_{AE}a_3(-\ln t_{q_k})}{\lambda_{AE}a_5(-\ln t_k)+\lambda_{AE}a_6}+\frac{m_{BE}}{\lambda_{BE}}\right)a_7}\sum_{i_4=0}^{i_2+m_{BE}-1}\frac{(i_2+m_{BE}-1)!}{i_4!}(a_7(-\ln t_k))^{i_4} \\
&\times\left(\frac{m_{AE}a_3(-\ln t_{q_k})}{\lambda_{AE}a_5(-\ln t_k)+\lambda_{AE}a_6}+\frac{m_{BE}}{\lambda_{BE}}\right)^{i_4-i_2-m_{BE}}\Bigg], \qquad (25)
\end{aligned}$$

where $a_3 = \Omega_S\gamma_5\gamma_1$, $a_4 = \Omega_S\gamma_6\gamma_1$, $a_5 = \gamma_4\gamma_2$, $a_6 = \gamma_3\gamma_4$, $a_7 = \frac{(\gamma_5\delta_{BE}+1)\Omega_S\gamma_2}{\gamma_5(\gamma_2\delta_{BU}+1)}$, $v_q = \cos\left(\frac{\pi(2r-1)}{2R}\right)$, $t_{qk} = \frac{b_k(v_q+1)}{2}$, $b_k = e^{-v_3}t_k{}^{v_2}$, *with* R *is the complexity versus accuracy trade-off coefficient [19].*

Proof. See Appendix B.

4 Numerical Result

In this section, the numerical results are provided to look insight the behaviors of our proposed system as well as to verify our analysis. In our work, we use Monte Carlo method to carry the simulations of UAV-assisted NOMA-MEC in IoT system. The simulation parameters are shown in Table 1 [2,14].

The impact of the average SNR γ_I and the channel estimation error δ_ψ on the SSCP and upper bound for the SSCP are depicted in Fig. 3. With this result, we

Table 1. Simulation parameter.

Parameter	Value	Parameter	Value	Parameter	Value
(x_A, y_A)	$(0, 50)$ (m)	$\mathcal{A}$	0.1581	P_S	$(0, 20)$ (dB)
(x_B, y_B)	$(40, 0)$ (m)	$\mathcal{B}$	9.6177	T	0.5 (s)
(x_E, y_E)	$(90, 90)$ (m)	$\mathcal{O}_{LoS}$	1	ρ	$(0.5, 1)$
x_U	0 (m)	$\mathcal{O}_{NLoS}$	20	σ	2
y_U	0 (m)	c	3.10^8 (m/s)	W	10^5 (Hz)
h_U	$(30, 90)$ (m)	f_c	10^5 (Hz)	(β_A, β_B)	(0.6,0.4)
L	10^4 (bit)	f_U^{MEC}	10^6 (Hz)	P_E	$(15, 25)$ (dB)
R	10^3	ς	3	R_s	8000 (bps/Hz)
$Q = K$	10^2	m_A, m_B, m_{AE}, m_{BE}	2	δ_ψ	(0,5)

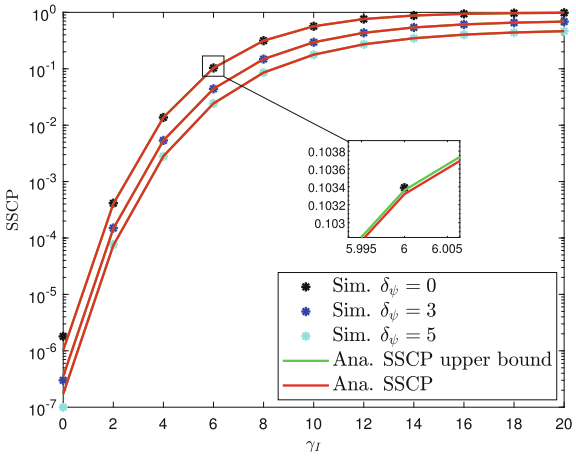

Fig. 3. SSCP vs. the average transmit SNR γ_I with different channel estimation error δ_ψ.

consider SSCP and its upper bound for cases of $\delta_\psi = 0$, i.e., perfect CSI (pCSI), $\delta_\psi = 3$ and $\delta_\psi = 5$. With $\delta_\psi = 0$, we see that SSCP as well as its upper bound are better than the other cases because this is the ideal case of the system. In practice, achieving pCSI is extremely difficult, so in our work we consider the case of iCSI for the practical system.

Figure 4 illustrates the impact of the UAV's altitude, h_U, and three different average SNR γ_E values on the SSCP of the entire system. It can be observed that a lower average SNR γ_E leads to better SSCP performance. We can also observe that there exists an optimal UAV altitude to maximize secrecy offloading performance, which can be explained by the fact that at lower UAV altitudes, the probability of encountering an NLoS is higher than an LoS due to urban obstacles. Increasing the UAV altitude improves performance because the prob-

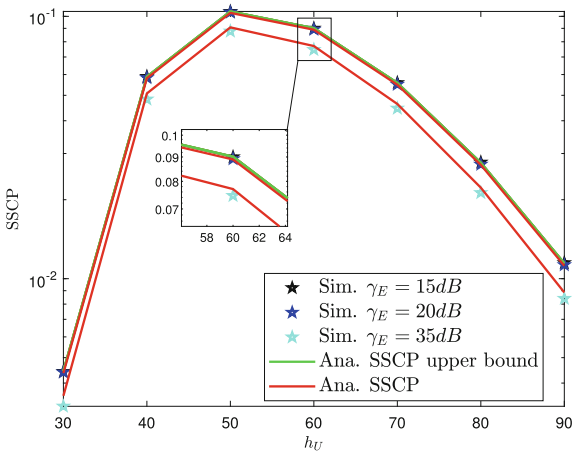

Fig. 4. SSCP vs. the altitude of UAV with three different average SNR γ_E values.

ability of encountering an LoS between the UAV and the ED is higher than encountering an NLoS. Nonetheless, the greater the altitude, the greater the communication distance between the UAV and the ED, which increases the pass loss of the UAV-ED links and consequently decreases the performance. So there will be an altitude that maximizes the efficacy of secrecy offloading.

In order to investigate the influence of transmit power on our system performance, we assume that the total transmit power (P_S) of two users is fixed and the power allocation ratio is used to allocate the transmit power for each user. Figure 5 depicts the curve of SSCP and its upper bound versus the power allo-

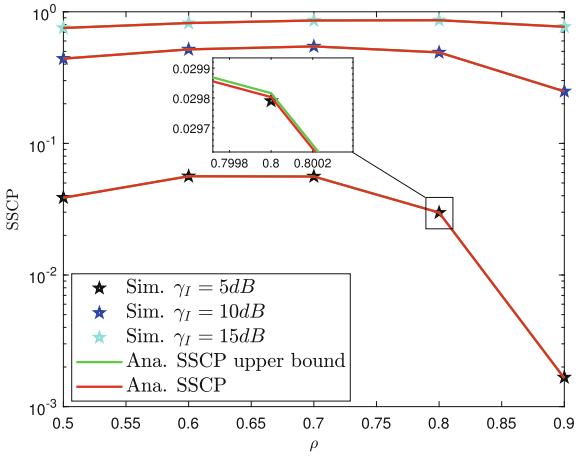

Fig. 5. SSCP vs. the power allocation ratio ρ with three different average SNR γ_I values.

cation ratio with different average SNR γ_I. From this figure, we can observe the existence of an optimal value, denoted as ρ^*, corresponding to the best achievable SSCP of the system. This indicates a trade-off between the secrecy performance and the latency of A and B.

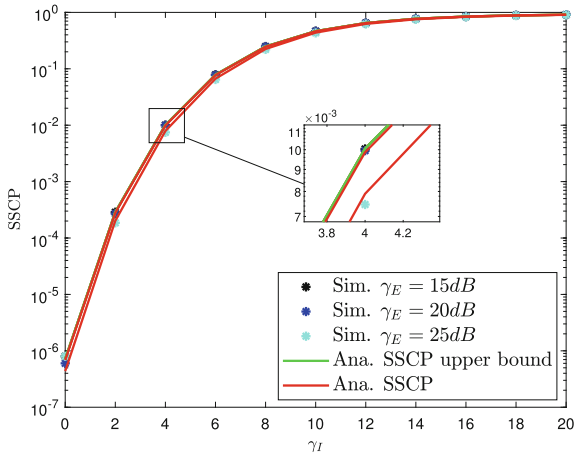

Fig. 6. SSCP vs. the average transmit SNR γ_I with different average transmit SNR γ_E values.

Figure 6 depicts the SSCP when varying the average SNR γ_E and the average SNR γ_I. It can be observed that an increase in γ_I leads to an improvement in the SSCP. This is because an increase in the average SNR γ_I indicates a better quality of the legitimate channel, thereby enhancing security against eavesdropping. This also explains why an increase in the average SNR γ_E of the eavesdropper's receiver results a decrease of SSCP.

We can observe that Monte Carlo simulation and our analysis have strong matching which confirms the accuracy of our analytic results.

5 Conclusion

In this paper, we have investigated the secrecy and latency performance of an UAV-assisted NOMA-MEC in IoT over Nakagami-m fading channels. A fourth-phase offloading protocol has been proposed based on UAV-aided with NOMA-MEC techniques to increase the secrecy offloading performance. The exact closed-form expressions of the SSCP and its upper-bound expressions are derived. The numerical results have been provided to look insight the behavior of this system and verified our analytical expressions. In order to improve the secrecy and latency performance of this system, we can increase the transmit power or/and control the UAV hovering on the optimal altitude or/and choose the best transmit power allocation ratio. In our future work, we will focus on the

performance optimization by finding the optimal trajectory of UAV according to the position of eavesdropper.

Acknowledgment. This research is funded by Vietnam National Foundation for Science and Technology Development (NAFOSTED) under grant number 102.04-2021.11.

A Proof of Theorem 1

By substituting (7), (8), (10), (11), (12), (13), (14), and (15) into (16), we can rewrite the $\mathcal{S}$ of system as

$$\begin{aligned}\mathcal{S} &= \Pr\left\{X > v_1, Y > v_2X + v_3, Z < v_4X + v_5, S < \Xi_1^{(X,Y)} + \Xi_2^{(X,Y)}\right\}, \\ &= \int_{v_1}^{\infty}\int_{v_2X+v_3}^{\infty}\int_{0}^{v_4X+v_5} F_S\left(\Xi_1^{(X,Y)} + \Xi_2^{(X,Y)}\right) f_Z(z)\, f_Y(y)\, f_X(x)\, dzdydx, \quad (26)\end{aligned}$$

where $X = |\hat{g}_{BU}|^2$, $Y = |\hat{g}_{AU}|^2$, $Z = |\hat{g}_{BE}|^2$, $S = |\hat{g}_{AE}|^2$, $\theta_A = 2^{\frac{L_A^{off}}{WT^{th}}} - 1$, $\theta_B = 2^{\frac{L_B^{off}}{WT^{th}}} - 1$, $\varphi_S = 2^{\frac{R_S}{W}}$, $v_1 = \frac{\theta_B(\gamma_2\delta_{BU}+1)}{\gamma_2}$, $v_2 = \frac{\theta_A\gamma_2}{\gamma_1}$, $v_3 = \frac{\theta_A\gamma_3}{\gamma_1}$, $v_4 = \frac{\gamma_2(\gamma_5\delta_{BE}+1)}{\gamma_5\varphi_S(\gamma_2\delta_{BU}+1)}$, $v_5 = \frac{(1-\varphi_S)(\gamma_5\delta_{BE}+1)}{\gamma_5\varphi_S}$, $\Xi_1^{(X,Y)} = \left(\frac{\gamma_1 Y}{\gamma_2 X+\gamma_3} + 1 - \varphi_S\right)\frac{\gamma_5}{\gamma_4\varphi_S}$, and $\Xi_2^{(X,Y)} = \left(\frac{\gamma_1 Y}{\gamma_2 X+\gamma_3} + 1 - \varphi_S\right)\frac{\gamma_6}{\gamma_4\varphi_S}$ There are three integrals here, so we do the integration one by one. First, we solve the 1st integral, denoted by $\mathcal{I}_1$. By combining the CDF in (4) and the PDF in (5) into $\mathcal{I}_1$, we can rewrite as follow:

$$\begin{aligned}\mathcal{I}_1 = \frac{m_{BE}^{m_{BE}}}{\lambda_{BE}^{m_{BE}}(m_{BE}-1)!}\Bigg[&\int_0^{v_4X+v_5} z^{m_{BE}-1}e^{-\frac{m_{BE}z}{\lambda_{BE}}}dz - \sum_{i_1=0}^{m_{AE}-1}\frac{1}{i_1!}\left(\frac{m_{AE}}{\lambda_{AE}}\right)^{i_1} \\ &\times \int_0^{v_4X+v_5} z^{m_{BE}-1}e^{-\frac{m_{AE}}{\lambda_{AE}}\left(\Xi_1^{(X,Y)}z+\Xi_2^{(X,Y)}\right)-\frac{m_{BE}z}{\lambda_{BE}}}\left(\Xi_1^{(X,Y)}z + \Xi_2^{(X,Y)}\right)^{i_1}dz\Bigg]. \quad (27)\end{aligned}$$

After a few mathematical transformations, the integrals in formula 28 are solved by applying the Eq. (3.351.1[8]) in [21] shown in (28).

$$\mathcal{I}_1 = \frac{m_{BE}^{m_{BE}}}{\lambda_{BE}^{m_{BE}}(m_{BE}-1)!}\left(\mathcal{I}_{11} - \mathcal{I}_{12} - \mathcal{I}_{13}\right), \quad (28)$$

where $\mathcal{I}_{11}$, $\mathcal{I}_{12}$, and $\mathcal{I}_{13}$ are define as follow:

$$\mathcal{I}_{11} = (m_{BE}-1)!\left(\frac{m_{BE}}{\lambda_{BE}}\right)^{-m_{BE}}, \tag{29}$$

$$\mathcal{I}_{12} = e^{-\frac{m_{BE}(v_4X+v_5)}{\lambda_{BE}}} \sum_{i_2=0}^{m_{BE}-1} \frac{(m_{BE}-1)!}{i_2!}\left(\frac{m_{BE}}{\lambda_{BE}}\right)^{-(m_{BE}-i_2)} (v_4X+v_5)^{i_2}, \tag{30}$$

$$\begin{aligned}\mathcal{I}_{13} = &\sum_{i_1=0}^{m_{AE}-1}\sum_{i_3=0}^{i_1} \frac{1}{i_3!\,(i_1-i_3)!}\left(\frac{m_{AE}}{\lambda_{AE}}\right)^{i_1}\left(\frac{\gamma_6}{\gamma_5}\right)^{i_1-i_3}\left(\Xi_1^{(X,Y)}\right)^{i_1} e^{-\frac{m_{AE}}{\lambda_{AE}}\Xi_2^{(X,Y)}}\\ &\times\left[(m_{BE}+i_3-1)!\left(\Xi_3^{(X,Y)}\right)^{-(m_{BE}+i_3)} - e^{-\left(\frac{m_{AE}\Xi_1^{(X,Y)}}{\lambda_{AE}}+\frac{m_{BE}}{\lambda_{BE}}\right)(v_4X+v_5)}\right.\\ &\times\left.\sum_{i_4=0}^{m_{BE}+i_3-1}\frac{(m_{BE}+i_3-1)!}{i_4!}(v_4X+v_5)^{i_4}\left(\Xi_3^{(X,Y)}\right)^{-(m_{BE}+i_3-i_4)}\right],\end{aligned} \tag{31}$$

where $\Xi_3^{(X,Y)} = \left(\frac{m_{AE}\Xi_1^{(X,Y)}}{\lambda_{AE}}+\frac{m_{BE}}{\lambda_{BE}}\right)$. Next, we substitute $\mathcal{I}_1$ in (28) and the PDF in (5) into the 2nd integral, denoted by $\mathcal{I}_2$, which can be expressed as follows:

$$\begin{aligned}\mathcal{I}_2 = &\frac{m_A^{m_A}}{\lambda_A^{m_A}\,(m_A-1)!}\frac{m_{BE}^{m_{BE}}}{\lambda_{BE}^{m_{BE}}\,(m_{BE}-1)!}\left[\underbrace{(\mathcal{I}_{11}-\mathcal{I}_{12})\int_{v_2X+v_3}^{\infty} y^{m_A-1}e^{-\frac{m_A y}{\lambda_A}}dy}_{\mathcal{I}_{21}}\right.\\ &-\sum_{i_1=0}^{m_{AE}-1}\sum_{i_3=0}^{i_1}\frac{(m_{BE}+i_3-1)!}{i_3!\,(i_1-i_3)!}\left(\frac{m_{AE}}{\lambda_{AE}}\right)^{i_1}\left(\frac{\gamma_6}{\gamma_5}\right)^{i_1-i_3}\\ &\times\int_{v_2X+v_3}^{\infty} y^{m_A-1}\left(\Xi_1^{(X,y)}\right)^{i_1}\left(\Xi_3^{(X,y)}\right)^{-(m_{BE}+i_3)} e^{-\frac{m_{AE}}{\lambda_{AE}}\Xi_2^{(X,y)}-\frac{m_A y}{\lambda_A}}\\ &\times\left.\underbrace{\left(1-e^{-\Xi_3^{(X,y)}(v_4X+v_5)}\sum_{i_4=0}^{m_{BE}+i_3-1}\frac{(v_4X+v_5)^{i_4}}{i_4!}\left(\Xi_3^{(X,y)}\right)^{i_4}\right)dy}_{\mathcal{I}_{22}}\right],\end{aligned} \tag{32}$$

From (32), for $\mathcal{I}_{21}$, we solve the integrals by Eq. $(3.351.1^{11})$ in [21], shown in (33). For $\mathcal{I}_{22}$, let $v = e^{-X}$ and $X = -\ln(v)$, then $\mathcal{I}_{22}$ solved using the

Gaussian-Chebyshev quadrature method [19], shown in (34).

$$\mathcal{I}_{21} = (\mathcal{I}_{11} - \mathcal{I}_{12})\, e^{-\frac{m_A(v_2X+v_3)}{\lambda_A}} \sum_{j_1=0}^{m_A-1} \frac{(m-1)!(v_2X+v_3)^{j_1}}{j_1!} \left(\frac{m_A}{\lambda_A}\right)^{-(m_A-j_1)}, \tag{33}$$

$$\begin{aligned}\mathcal{I}_{22} = {} & \frac{\pi}{2R} \sum_{i_1=0}^{m_{AE}-1} \sum_{i_3=0}^{i_1} \sum_{r=1}^{R} \frac{(m_{BE}+i_3-1)!\sqrt{1-\zeta_o^2}}{i_3!\,(i_1-i_3)!} \left(\frac{m_{AE}}{\lambda_{AE}}\right)^{i_1} \left(\frac{\gamma_6}{\gamma_5}\right)^{i_1-i_3} \\ & \times \left(\theta_o^{(X)}\right)^{m_A-1} \left(\omega_o^{(X)}\right)^{\frac{m_A}{\lambda_A}-1} \left(\Xi_1^{\left(X,\theta_o^{(X)}\right)}\right)^{i_1} \left(\Xi_3^{\left(X,\theta_o^{(X)}\right)}\right)^{-(m_{BE}+i_3)} \\ & \times e^{-\frac{m_{AE}}{\lambda_{AE}}\Xi_2^{\left(X,\theta_o^{(X)}\right)}-(v_2X+v_3)} \left(1 - e^{-\Xi_3^{\left(X,\theta_o^{(X)}\right)}(v_4X+v_5)}\right. \\ & \times \left.\sum_{i_4=0}^{m_{BE}+i_3-1} \frac{(v_4X+v_5)^{i_4}}{i_4!} \left(\Xi_3^{\left(X,\theta_o^{(X)}\right)}\right)^{i_4}\right),\end{aligned} \tag{34}$$

where $\zeta_o = \cos\left(\frac{\pi(2r-1)}{2R}\right)$, $\omega_o^{(X)} = \frac{(\zeta_o+1)e^{-(v_2X+v_3)}}{2}$, $\theta_o^{(X)} = -\ln\left(\omega_o^{(X)}\right)$, and R is the complexity versus accuracy trade-off coefficient. Finally, we Combining (33) and (34) into (32) and the PDF in (5) into the last integral in (27), then $\mathcal{S}$ is expressed as:

$$\mathcal{S} = \mathcal{C}\,(\mathcal{I}_{31} - \mathcal{I}_{32} - \mathcal{I}_{33}), \tag{35}$$

where $\mathcal{C} = \frac{m_A^{m_A}}{\lambda_A^{m_A}(m_A-1)!} \frac{m_B^{m_B}}{\lambda_B^{m_B}(m_B-1)!} \frac{m_{BE}^{m_{BE}}}{\lambda_{BE}^{m_{BE}}(m_{BE}-1)!}$; $\mathcal{I}_{31}$, $\mathcal{I}_{32}$ and $\mathcal{I}_{33}$ are defined as follows:

$$\begin{aligned}\mathcal{I}_{31} = {} & (m_{BE}-1)! \left(\frac{m_{BE}}{\lambda_{BE}}\right)^{-m_{BE}} \sum_{j_1=0}^{m_A-1} \frac{(m_A-1)!}{j_1!} \left(\frac{m_A}{\lambda_A}\right)^{-(m_A-j_1)} e^{-\frac{m_A v_3}{\lambda_A}} \\ & \times \int_{v_1}^{\infty} x^{m_B-1}(v_2x+v_3)^{j_1} e^{-\left(\frac{m_A v_2}{\lambda_A}+\frac{m_B}{\lambda_B}\right)x} dx,\end{aligned} \tag{36}$$

$$\begin{aligned}\mathcal{I}_{32} = {} & \sum_{i_2=0}^{m_{BE}-1} \sum_{j_1=0}^{m_A-1} \frac{(m_A-1)!}{j_1!} \frac{(m_{BE}-1)!}{i_2!} \left(\frac{m_{BE}}{\lambda_{BE}}\right)^{-(m_{BE}-i_2)} \left(\frac{m_A}{\lambda_A}\right)^{-(m_A-j_1)} \\ & \times \int_{v_1}^{\infty} x^{m_B-1}(v_2X+v_3)^{j_1}(v_4X+v_5)^{i_2} e^{-\frac{m_{BE}(v_4X+v_5)}{\lambda_{BE}} - \frac{m_A(v_2X+v_3)}{\lambda_A}} e^{-\frac{m_B x}{\lambda_B}} dx,\end{aligned} \tag{37}$$

$$\mathcal{I}_{33} = \frac{\pi}{2R}\sum_{i_1=0}^{m_{AE}-1}\sum_{i_3=0}^{i_1}\sum_{r=1}^{R}\frac{(m+i_3-1)!\sqrt{1-\zeta_o{}^2}}{i_3!(i_1-i_3)!}\left(\frac{m_{AE}}{\lambda_{AE}}\right)^{i_1}\left(\frac{\gamma_6}{\gamma_5}\right)^{i_1-i_3}$$
$$\times\int_{v_1}^{\infty}x^{m_B-1}\left(\theta_o^{(x)}\right)^{m_A-1}\left(\omega_o^{(x)}\right)^{\frac{m_A}{\lambda_A}-1}\left(\Xi_1^{\left(x,\theta_o^{(x)}\right)}\right)^{i_1}\left(\Xi_3^{\left(x,\theta_o^{(x)}\right)}\right)^{-(m_{BE}+i_3)}$$
$$\times e^{-\frac{m_{AE}}{\lambda_{AE}}\Xi_2^{\left(x,\theta_o^{(x)}\right)}}e^{-\frac{m_B x}{\lambda_B}-(v_2x+v_3)}\left(1-e^{-\Xi_3^{\left(x,\theta_o^{(x)}\right)}(v_4x+v_5)}\right.$$
$$\left.\times\sum_{i_4=0}^{m+i_3-1}\frac{(v_4x+v_5)^{i_4}}{i_4!}\left(\Xi_3^{\left(x,\theta_o^{(x)}\right)}\right)^{i_4}\right)dx, \tag{38}$$

Similar to the integral solution of $\mathcal{I}_2$. $\mathcal{I}_{31}$ and $\mathcal{I}_{32}$ are expressed as follows:

$$\mathcal{I}_{31} = (m_{BE}-1)!\left(\frac{m_{BE}}{\lambda_{BE}}\right)^{-m_{BE}}\sum_{j_1=0}^{m_A-1}\sum_{k_1=0}^{j_1}\sum_{k_2=0}^{m_B+k_1-1}\frac{(m_B+k_1-1)!}{k_2!k_1!\,(j_1-k_1)!}$$
$$\times(m_A-1)!\left(\frac{m_A}{\lambda_A}\right)^{-(m_A-j_1)}\left(\frac{v_3}{v_2}\right)^{j_1-k_1}\left(\frac{m_Av_2}{\lambda_A}+\frac{m_B}{\lambda_B}\right)^{-(m_B+k_1-k_2)}$$
$$\times {v_2}^{j_1}{v_1}^{k_2}e^{-v_1\left(\frac{m_Av_2}{\lambda_A}+\frac{m_B}{\lambda_B}\right)-\frac{m_Av_3}{\lambda_A}}, \tag{39}$$

$$\mathcal{I}_{32} = \sum_{i_2=0}^{m_{BE}-1}\sum_{j_1=0}^{m_A-1}\sum_{k_1=0}^{j_1}\sum_{k_3=0}^{i_2}\sum_{k_4=0}^{m_B+k_1+k_3-1}\left(\frac{m_{BE}}{\lambda_{BE}}\right)^{-(m_{BE}-i_2)}\left(\frac{m_A}{\lambda_A}\right)^{-(m_A-j_1)}$$
$$\times\frac{(m_A-1)!\,(m_{BE}-1)!\,(m_B+k_1+k_3-1)!}{k_1!k_3!k_4!(j_1-k_1)!(i_2-k_3)!}\left(\frac{v_3}{v_2}\right)^{j_1-k_1}\left(\frac{v_5}{v_4}\right)^{i_2-k_3}$$
$$\times\left(\frac{m_{BE}v_4}{\lambda_{BE}}+\frac{m_Av_2}{\lambda_A}+\frac{m_B}{\lambda_B}\right)^{-(m_B+k_1+k_3-k_4)}{v_1}^{k_4}{v_2}^{j_1}{v_4}^{i_2}$$
$$\times e^{-\left(\frac{m_{BE}v_4}{\lambda_{BE}}+\frac{m_Av_2}{\lambda_A}+\frac{m_B}{\lambda_B}\right)v_1+\frac{m_{BE}v_5}{\lambda_{BE}}+\frac{m_Av_3}{\lambda_A}}, \tag{40}$$

$$\mathcal{I}_{33} = \frac{\pi^2}{4QR}\sum_{i_1=0}^{m_{AE}-1}\sum_{i_3=0}^{i_1}\sum_{r=1}^{R}\sum_{q=1}^{Q}\left(\frac{m_{AE}}{\lambda_{AE}}\right)^{i_1}\left(\frac{\gamma_6}{\gamma_5}\right)^{i_1-i_3}(\theta_q)^{m_B-1}\left(\theta_o^{(\theta_q)}\right)^{m_A-1}$$
$$\times\frac{(m_{BE}+i_3-1)!\sqrt{1-\zeta_q{}^2}\sqrt{1-\zeta_o{}^2}}{i_3!\,(i_1-i_3)!}\omega_q{}^{\frac{m_B}{\lambda_B}-1}\left(\omega_o^{(\theta_q)}\right)^{\frac{m_A}{\lambda_A}-1}$$
$$\times\left(\Xi_1^{\left(\theta_q,\theta_o^{(\theta_q)}\right)}\right)^{i_1}\left(\Xi_3^{\left(\theta_q,\theta_o^{(\theta_q)}\right)}\right)^{-(m_{BE}+i_3)}e^{-\frac{m_{AE}}{\lambda_{AE}}\Xi_2^{\left(\theta_q,\theta_o^{(\theta_q)}\right)}-(v_2\theta_q+v_3)}$$
$$\times\left[1-e^{-\Xi_3^{\left(\theta_q,\theta_o^{(\theta_q)}\right)}(v_4\theta_q+v_5)}\sum_{i_4=0}^{m_{BE}+i_3-1}\frac{1}{i_4!}(v_4\theta_q+v_5)^{i_4}\left(\Xi_3^{\left(\theta_q,\theta_o^{(\theta_q)}\right)}\right)^{i_4}\right], \tag{41}$$

where $\zeta_q = \cos\left(\frac{\pi(2q-1)}{2Q}\right)$, $\omega_q = \frac{(\zeta_q+1)e^{-v_1}}{2}$, and $\theta_q = -\ln(\omega_q)$ with Q is the complexity versus accuracy trade-off coefficient. By substituting (39), (40) and

(41) into (35), we obtain a closed-form expression for the SSCP of the entire system as in Theorem 1.

B Proof of Theorem 2

$$\begin{aligned}\mathcal{S} &= \Pr\left(t_{AU}^{off} < T^{th}, t_{BU}^{off} < T^{th}, C_{AU}^{\text{Sec}} > R_S, C_{BU}^{\text{Sec}} > R_S\right) \\ &< \mathcal{S}_{upper} = \Pr\left(\gamma_A > \theta_A, \gamma_B > \theta_B, \gamma_{EA} < \Omega_S\gamma_A, \gamma_{EB} < \Omega_S\gamma_B\right), \end{aligned} \tag{42}$$

where $\Omega_S = 1/2^{\frac{R_S}{W}}$.

$$\begin{aligned}\mathcal{S}_{upper} &= \Pr\left(X > v_2Y + v_3, Y > v_1, S < \frac{a_3XZ + a_4X}{a_5Y + a_6}, Z < a_7Y\right) \\ &= \underbrace{\int_{v_1}^{\infty} f_Y(y) \underbrace{\int_{v_2y+v_3}^{\infty} f_X(x) \underbrace{\int_0^{a_7y} F_S\left[\frac{a_3xz + a_4x}{a_5y + a_6}\right] f_Z(z)\, dz}_{I_1}\, dx}_{I_2}\, dy}_{I_3}, \end{aligned} \tag{43}$$

where $X = |\hat{g}_{AU}|^2$, $Y = |\hat{g}_{BU}|^2$, $Z = |\hat{g}_{BE}|^2$, $S = |\hat{g}_{AE}|^2$. There are three integrals here, so we do the integration one by one. First, we solve the 1st integral, denoted by I_1. By combining the CDF in (4) and the PDF in (5) into I_1, we can rewrite as follow:

$$\begin{aligned} I_1 = &\underbrace{\int_0^{a_7y} \frac{1}{(m_{BE}-1)!}\left(\frac{m_{BE}}{\lambda_{BE}}\right)^{m_{BE}} z^{m_{BE}-1} e^{-\frac{m_{BE}}{\lambda_{BE}}z} dz}_{I_{11}} - \frac{1}{(m_{BE}-1)!}\left(\frac{m_{BE}}{\lambda_{BE}}\right)^{m_{BE}} \\ &\times e^{-\frac{m_{AE}a_4x}{\lambda_{AE}a_5y+\lambda_{AE}a_6}} \sum_{i_1=0}^{m_{AE}-1} \frac{1}{i_1!}\left(\frac{m_{AE}}{\lambda_{AE}}\right)^{i_1}\left(\frac{a_3x}{a_5y+a_6}\right)^{i_1} \sum_{i_2=0}^{i_1} C_{i_2}^{i_1}\left(\frac{a_4}{a_3}\right)^{i_1-i_2} \\ &\times \underbrace{\int_0^{a_7y} e^{-\left(\frac{m_{AE}a_3x}{\lambda_{AE}a_5y+\lambda_{AE}a_6}+\frac{m_{BE}}{\lambda_{BE}}\right)z} z^{i_2+m_{BE}-1} dz}_{I_{12}}, \end{aligned} \tag{44}$$

After a few mathematical transformations, the integrals in formula 44 are solved by applying the Eq. ($3.351.1^8$) in [21].

$$I_{11} = 1 - e^{-\frac{m_{BE}}{\lambda_{BE}}a_7y} \sum_{i_3=0}^{m_{BE}-1} \frac{1}{i_3!}\left(\frac{m_{BE}}{\lambda_{BE}}a_7y\right)^{i_3}, \tag{45}$$

$$I_{12} = (i_2 + m_{BE} - 1)!\left(\frac{m_{AE}a_3 x}{\lambda_{AE}a_5 y + \lambda_{AE}a_6} + \frac{m_{BE}}{\lambda_{BE}}\right)^{-i_2 - m_{BE}} - \sum_{i_4=0}^{i_2+m_{BE}-1} (a_7 y)^{i_4}$$
$$\times\, e^{-\left(\frac{m_{AE}a_3 x}{\lambda_{AE}a_5 y + \lambda_{AE}a_6} + \frac{m_{BE}}{\lambda_{BE}}\right)a_7 y} \frac{(i_2 + m_{BE} - 1)!}{i_4!}\left(\frac{m_{AE}a_3 x}{\lambda_{AE}a_5 y + \lambda_{AE}a_6} + \frac{m_{BE}}{\lambda_{BE}}\right)^{i_4 - i_2 - m_{BE}}, \tag{46}$$

Next, we substitute I_1 in (29) and the PDF in (5) into the 2nd integral, denoted by I_2, which can be expressed as follows:

$$I_2 = \underbrace{\int_{v_2 y + v_3}^{\infty} f_{g_A}(x)\, dx}_{I_{21}} - e^{-\frac{m_{BE}}{\lambda_{BE}}a_7 y} \sum_{i_3=0}^{m_{BE}-1} \frac{1}{i_3!}\left(\frac{m_{BE}}{\lambda_{BE}}a_7 y\right)^{i_3} \underbrace{\int_{v_2 y + v_3}^{\infty} f_{g_A}(x)\, dx}_{I_{21}}$$
$$- \frac{1}{(m_{BE}-1)!}\left(\frac{m_{BE}}{\lambda_{BE}}\right)^{m_{BE}} \sum_{i_1=0}^{m_{AE}-1} \frac{1}{i_1!}\left(\frac{m_{AE}}{\lambda_{AE}}\left(\frac{a_3}{a_5 y + a_6}\right)\right)^{i_1} \sum_{i_2=0}^{i_1} C_{i_2}^{i_1}\left(\frac{a_4}{a_3}\right)^{i_1 - i_2}$$
$$\times \underbrace{\int_{v_2 y + v_3}^{\infty} f_{g_A}(x)\, dx e^{-\frac{m_{AE}a_4 x}{\lambda_{AE}a_5 y + \lambda_{AE}a_6}} x^{i_1}}_{I_{22}} [(i_2 + m_{BE} - 1)!$$
$$\times \left(\frac{m_{AE}a_3 x}{\lambda_{AE}a_5 y + \lambda_{AE}a_6} + \frac{m_{BE}}{\lambda_{BE}}\right)^{-i_2 - m_{BE}} - e^{-\left(\frac{m_{AE}a_3 x}{\lambda_{AE}a_5 y + \lambda_{AE}a_6} + \frac{m_{BE}}{\lambda_{BE}}\right)a_7 y}$$
$$\times \sum_{i_4=0}^{i_2+m_{BE}-1} \frac{(i_2 + m_{BE} - 1)!}{i_4!}(a_7 y)^{i_4}\left(\frac{m_{AE}a_3 x}{\lambda_{AE}a_5 y + \lambda_{AE}a_6} + \frac{m_{BE}}{\lambda_{BE}}\right)^{i_4 - i_2 - m_{BE}}], \tag{47}$$

From (47), for I_{21}, we solve the integrals by the CDF in (4). For I_{22}, let $\rho = e^{-x}$ and $x = -\ln(\rho)$, then I_{22} solved using the Gaussian-Chebyshev quadrature method [19], shown in (49).

$$I_{21} = e^{-\frac{m_A}{\lambda_A}(v_2 y + v_3)} \sum_{i_5=0}^{m_A - 1} \frac{1}{i_5!}\left(\frac{m_A}{\lambda}(v_2 y + v_3)\right)^{i_5}, \tag{48}$$

$$I_{22} = \frac{1}{(m_A - 1)!}\left(\frac{m_A}{\lambda_A}\right)^{m_A} \frac{\pi}{R} \sum_{r=0}^{R} \frac{\sqrt{1 - v_q}}{\sqrt{1 + v_q}} t_{q[y]}\, \frac{m_{AE}a_4}{\lambda_{AE}a_5 y + \lambda_{AE}a_6} + \frac{m_A}{\lambda_A}$$
$$\times \left(-\ln t_{q[y]}\right)^{i_1 + m_A - 1}\left[(i_2 + m_{BE} - 1)!\left(\frac{m_{AE}a_3\left(-\ln t_{q[y]}\right)}{\lambda_{AE}a_5 y + \lambda_{AE}a_6} + \frac{m_{BE}}{\lambda_{BE}}\right)^{-i_2 - m_{BE}}\right.$$
$$- e^{-\left(\frac{m_{AE}a_3\left(-\ln t_{q[y]}\right)}{\lambda_{AE}a_5 y + \lambda_{AE}a_6} + \frac{m_{BE}}{\lambda_{BE}}\right)a_7 y} \sum_{i_4=0}^{i_2+m_{BE}-1} \frac{(i_2 + m_{BE} - 1)!}{i_4!}(a_7 y)^{i_4}$$
$$\left.\times \left(\frac{m_{AE}a_3\left(-\ln t_{q[y]}\right)}{\lambda_{AE}a_5 y + \lambda_{AE}a_6} + \frac{m_{BE}}{\lambda_{BE}}\right)^{i_4 - i_2 - m_{BE}}\right], \tag{49}$$

where $v_q = \cos\left(\frac{\pi(2r-1)}{2R}\right)$, $t_{q_{[y]}} = \frac{b_{[y]}(v_q+1)}{2}$, $b_{[y]} = e^{-v_2 y - v_3}$, and R is the complexity versus accuracy trade-off coefficient. Finally, we Combining (48) and (49) into (47) and the PDF in (5) into the last integral in (43), then $\mathcal{S}_{upper}$ is expressed as:

$$\mathcal{S}_{upper} = \frac{1}{(m_B-1)!}\left(\frac{m_B}{\lambda_B}\right)^{m_B}\int_{v_1}^{\infty} y^{m_B-1}e^{-\frac{m_B}{\lambda_B}y}\left[e^{-\frac{m_A}{\lambda_A}(v_2y+v_3)}\sum_{i_5=0}^{m_A-1}\frac{1}{i_5!}\right.$$
$$\times\left(\frac{m_A}{\lambda_A}(v_2y+v_3)\right)^{i_5}\left[1-e^{-\frac{m_{BE}}{\lambda_{BE}}a_7y}\sum_{i_3=0}^{m_{BE}-1}\frac{1}{i_3!}\left(\frac{m_{BE}}{\lambda_{BE}}a_7y\right)^{i_3}\right]-\left(\frac{1}{(m_A-1)!}\right)$$
$$\times\left(\frac{1}{(m_{BE}-1)!}\right)\left(\frac{m_A}{\lambda_A}\right)^{m_A}\left(\frac{m_{BE}}{\lambda_{BE}}\right)^{m_{BE}}\frac{\pi}{R}\sum_{i_1=0}^{m_{AE}-1}\sum_{i_2=0}^{i_1}\sum_{r=0}^{R}\frac{\sqrt{1-v_q}}{\sqrt{1+v_q}}C_{i_2}^{i_1}\left(\frac{a_4}{a_3}\right)^{i_1-i_2}$$
$$\times\frac{1}{i_1!}\left(\frac{m_{AE}}{\lambda_{AE}}\left(\frac{a_3}{a_5y+a_6}\right)\right)^{i_1}t_{q_{[y]}}{}^{\frac{m_{AE}a_4}{\lambda_{AE}a_5y+\lambda_{AE}a_6}+\frac{m_A}{\lambda_A}}\left(-\ln t_{q_{[y]}}\right)^{i_1+m_A-1}$$
$$\times\left((i_2+m_{BE}-1)!\left(\frac{m_{AE}a_3\left(-\ln t_{q_{[y]}}\right)}{\lambda_{AE}a_5y+\lambda_{AE}a_6}+\frac{m_{BE}}{\lambda_{BE}}\right)^{-i_2-m_{BE}}\right.$$
$$\left.-e^{-\left(\frac{m_{AE}a_3\left(-\ln t_{q_{[y]}}\right)}{\lambda_{AE}a_5y+\lambda_{AE}a_6}+\frac{m_{BE}}{\lambda_{AE}}\right)a_7y}\sum_{i_4=0}^{i_2+m_{BE}-1}\frac{(i_2+m_{BE}-1)!}{i_4!}(a_7y)^{i_4}\right.$$
$$\left.\times\left(\frac{m_{AE}a_3\left(-\ln t_{q_{[y]}}\right)}{\lambda_{AE}a_5y+\lambda_{AE}a_6}+\frac{m_{BE}}{\lambda_{BE}}\right)^{i_4-i_2-m_{BE}}\right)\Bigg]dy, \tag{50}$$

Similar to the integral solution of I_2, we obtain an upper-bound expression for the SSCP of the entire system as given in Theorem 2. The proof is completed.

References

1. Li, B., Wu, W., Zhao, W., Zhang, H.: Security enhancement with a hybrid cooperative NOMA scheme for MEC system. IEEE Trans. Veh. Technol. **70**(3), 2635–2648 (2021)
2. Nguyen, A.-N., Ha, D.-B., Vo, V.N., Truong, V.-T., Do, D.-T., So-In, C.: Performance analysis and optimization for IoT mobile edge computing networks with RF energy harvesting and UAV relaying. IEEE Access **10**, 21 526–21 540 (2022)
3. Nguyen, A.-N., Vo, V.N., So-In, C., Ha, D.-B.: System performance analysis for an energy harvesting IoT system using a DF/AF UAV-enabled relay with downlink NOMA under Nakagami-m fading. Sensors **21**(1), 285 (2021)
4. Xu, Y., Zhang, T., Loo, J., Yang, D., Xiao, L.: Completion time minimization for UAV-assisted mobile-edge computing systems. IEEE Trans. Veh. Technol. **70**(11), 12253–12259 (2021)
5. Ding, Z., Fan, P., Poor, H.V.: Impact of non-orthogonal multiple access on the offloading of mobile edge computing. IEEE Trans. Commun. **67**(1), 375–390 (2019)

6. Truong, V.-T., Vo, V.N., Ha, D.-B., So-In, C.: On the system performance of mobile edge computing in an uplink NOMA WSN with a multiantenna access point over nakagami-m fading. IEEE/CAA J. Autom. Sinica **9**(4), 668–685 (2022)
7. Guo, Y., You, C., Yin, C., Zhang, R.: UAV trajectory and communication co-design: flexible path discretization and path compression. IEEE J. Sel. Areas Commun. **39**(11), 3506–3523 (2021)
8. Liu, D., et al.: Opportunistic UAV utilization in wireless networks: motivations, applications, and challenges. IEEE Commun. Mag. **58**(5), 62–68 (2020)
9. Peng, H., Shen, X.: Multi-agent reinforcement learning based resource management in MEC- and UAV-assisted vehicular networks. IEEE J. Sel. Areas Commun. **39**(1), 131–141 (2021)
10. Nguyen, A.-N., Vo, V.N., So-In, C., Ha, D.-B., Truong, V.-T.: Performance analysis in UAV-enabled relay with NOMA under Nakagami-m fading considering adaptive power splitting. In: Proceedings of International Joint Conference on Computer Science and Software Engineering (JCSSE), pp. 1–6 (2021)
11. Zhou, X., McKay, M.R., Maham, B., Hjørungnes, A.: Rethinking the secrecy outage formulation: a secure transmission design perspective. IEEE Commun. Lett. **15**(3), 302–304 (2011)
12. Han, S., et al.: Energy efficient secure computation offloading in NOMA-based mMTC networks for IoT. IEEE Internet Things J. **6**(3), 5674–5690 (2019)
13. Wu, W., Zhou, F., Hu, R.Q., Wang, B.: Energy-efficient resource allocation for secure NOMA-enabled mobile edge computing networks. IEEE Trans. Commun. **68**(1), 493–505 (2020)
14. Nguyen, A.-N., et al.: On secrecy analysis of UAV-enabled relaying NOMA systems with RF energy harvesting. In: Proceedings of the Industrial Networks and Intelligent Systems, pp. 267–281, June 2022
15. Yang, Z., Ding, Z., Fan, P., Karagiannidis, G.K.: On the performance of non-orthogonal multiple access systems with partial channel information. IEEE Trans. Commun. **64**(2), 654–667 (2016)
16. Gao, Y., Xia, B., Liu, Y., Yao, Y., Xiao, K., Lu, G.: Analysis of the dynamic ordered decoding for uplink NOMA systems with imperfect CSI. IEEE Trans. Veh. Technol. **67**(7), 6647–6651 (2018)
17. Nguyen, A.-N., Nhan Vo, V., So-In, C., Ha, D.-B., Sanguanpong, S., Baig, Z.A.: On secure wireless sensor networks with cooperative energy harvesting relaying. IEEE Access **7**, 139 212–139 225 (2019)
18. Truong, V.-T., Ha, D.-B.: A novel secrecy offloading in NOMA heterogeneous mobile edge computing network. In: Proceedings of the Advanced Engineering - Theory and Applications, pp. 468–477, December 2022
19. Judd, K.L.: Quadrature methods presented at university of Chicago's initiative for computational economics (2012)
20. Kudathanthirige, D., Gunasinghe, D., Amarasuriya, G.: Performance analysis of intelligent reflective surfaces for wireless communication. In: ICC 2020 - 2020 IEEE International Conference on Communications (ICC), pp. 1–6, July 2020
21. Gradshteyn, I., Ryzhik, I.: Table of Integrals, Series, and Products. Academic Press, Burlington (2014). A. Jeffrey and D. Zwillinger, Eds